



Articles by College of Natural and Applied Sciences Faculty

2006

Identification of a Novel Inhibitory Actin-capping Protein Binding Motif in CD2-associated Protein

Serawit Bruck

Tobias B. Huber

Robert J. Ingham

Kyoungtae Kim

Hanspeter Niederstrasser

See next page for additional authors

Follow this and additional works at: <https://bearworks.missouristate.edu/articles-cnas>

Recommended Citation

Bruck, Serawit, Tobias B. Huber, Robert J. Ingham, Kyoungtae Kim, Hanspeter Niederstrasser, Paul M. Allen, Tony Pawson, John A. Cooper, and Andrey S. Shaw. "Identification of a novel inhibitory actin-capping protein binding motif in CD2-associated protein." *Journal of Biological Chemistry* 281, no. 28 (2006): 19196-19203.

This article or document was made available through BearWorks, the institutional repository of Missouri State University. The work contained in it may be protected by copyright and require permission of the copyright holder for reuse or redistribution.

For more information, please contact [BearWorks@library.missouristate.edu](mailto: BearWorks@library.missouristate.edu).

Authors

Serawit Bruck, Tobias B. Huber, Robert J. Ingham, Kyoungtae Kim, Hanspeter Niederstrasser, Paul M. Allen, Tony Pawson, John A. Cooper, and Andrey S. Shaw

Identification of a Novel Inhibitory Actin-capping Protein Binding Motif in CD2-associated Protein*

Received for publication, January 6, 2006, and in revised form, May 11, 2006. Published, JBC Papers in Press, May 16, 2006, DOI 10.1074/jbc.M600166200

Serawit Bruck^{‡§}, Tobias B. Huber[‡], Robert J. Ingham^{||}, Kyoungtae Kim^{||}, Hanspeter Niederstrasser^{||}, Paul M. Allen[‡], Tony Pawson^{||}, John A. Cooper^{||}, and Andrey S. Shaw^{‡1}

From the [‡]Department of Pathology and Immunology, [§]Graduate Program in Molecular Biophysics, ^{||}Department of Cell Biology and Physiology, Washington University School of Medicine, St. Louis, Missouri 63110 and ^{||}Samuel Lunenfeld Research Institute, Mount Sinai Hospital, Toronto, Ontario M5G 1X5, Canada

CD2-associated protein (CD2AP) is a scaffold molecule that plays a critical role in the maintenance of the kidney filtration barrier. Little, however, is understood about its mechanism of function. We used mass spectrometry to identify CD2AP-interacting proteins. Many of the proteins that we identified suggest a role for CD2AP in endocytosis and actin regulation. To address the role of CD2AP in regulation of the actin cytoskeleton, we focused on characterizing the interaction of CD2AP with actin-capping protein CP. We identified a novel binding motif LHXHTXXRPK(X)₆P present in CD2AP that is also found in its homolog Cin85 and other capping protein-associated proteins such as CARMIL and CKIP-1. CD2AP inhibits the function of capping protein *in vitro*. Therefore, our results support a role of CD2AP in the regulation of the actin cytoskeleton.

CD2-associated protein (CD2AP)² is a 70-kDa protein that was originally cloned as a protein that interacts with the cytoplasmic tail of CD2, a T lymphocyte and natural killer cell transmembrane protein (1). It is composed of three Src homology 3 (SH3) domains at the NH₂ terminus followed by proline-rich sequences and a coiled-coil domain at the extreme COOH terminus. It is expressed in all tissues except brain. Interestingly, CD2AP-deficient animals die of renal failure ~6 weeks of age (2). In the kidney, CD2AP is highly expressed in the glomerular epithelial cell, and it is implicated to play a role in a specialized cell junction known as a slit diaphragm (3).

A homolog of CD2AP, Cin85, was cloned as an interacting protein with the E3 ubiquitin ligase c-cbl (4) and as an inhibitor of phosphatidylinositol 3-kinase (5). Recently, several endocytic and actin-associated molecules have been reported to interact with CD2AP and Cin85. Some proteins have been demonstrated to interact with both CD2AP and Cin85, whereas others have only been shown to bind one or the other. CD2AP

has been shown to play a role in vesicular trafficking because of interactions with c-cbl and an active form of Rab4 (6). Cin85 has also been shown to bind to molecules involved in endocytosis, such as endophilin, synaptojanin 2B1, and SHIP-1 and the clathrin scaffold HIP1R (7, 8). Both CD2AP and Cin85 contain a motif, FXDXF, that mediates interactions with the α -appendage of clathrin adaptor protein 2 (9). Interactions of CD2AP and Cin85 with the phosphatidylinositol bisphosphate-dependent GTPase for ARF1 and ARF5, known as ASAP1, as well as cortactin- and actin-capping protein suggest additional roles in the regulation of the actin cytoskeleton (7, 10–12).

To further elucidate the molecular mechanism of CD2AP function, we performed mass spectrometry to identify interacting proteins. We identified novel and previously known interacting proteins such as actin-capping protein CP (11).

Over the last decade, there has been much progress in our understanding of how the actin cytoskeleton is regulated. Critical is the polymerization of monomeric G-actin to forming an asymmetric actin filament with a barbed and a pointed end. The barbed end is favored for polymerization. The Arp2/3 complex and formins can nucleate actin polymerization by creating free barbed ends, whereas gelsolin and actin-capping protein CP cap the barbed end (13, 14).

CP is a ubiquitously expressed heterodimer of α and β subunits (15). It is enriched in lamellipodia, and it plays an important role in cell motility (13). CP binds to the barbed end of the actin filament and prevents the addition and removal of actin subunits (16). By limiting the growth of pre-existing actin filaments, CP enhances new actin filament branching by the Arp2/3 complex (17). Recently, several proteins (CARMIL, CKIP-1, and V-1) have been demonstrated to bind and inhibit CP activity (18–20).

To understand the role of CD2AP in actin cytoskeleton dynamics, we decided to focus on characterizing the interaction of CD2AP with CP. Even though this interaction was previously reported (11), the mode of binding and the effect of CD2AP on the activity of CP are not known. In this report, we confirmed the binding of CD2AP with CP, and we mapped the interaction. This allowed us to identify a novel capping protein binding motif recognized by CP that is present in CD2AP, Cin85, CKIP-1, and CARMIL.

EXPERIMENTAL PROCEDURES

Co-immunoprecipitation—Co-immunoprecipitations were performed as described previously (21). Briefly, HEK293T cells

* This work was supported by National Institutes of Health Grant DK066428-AS and Biophysics Training Grant T32 GM08492. The costs of publication of this article were defrayed in part by the payment of page charges. This article must therefore be hereby marked "advertisement" in accordance with 18 U.S.C. Section 1734 solely to indicate this fact.

¹ To whom correspondence should be addressed: Dept. of Pathology and Immunology, Washington University School of Medicine, St. Louis, MO 63110. Tel.: 314-362-4614; Fax: 314-747-4888; E-mail: shaw@pathology.wustl.edu.

² The abbreviations used are: CD2AP, CD2-associated protein; GST, glutathione S-transferase; SH, Src homology; HEK, human embryonic kidney; HPLC, high pressure liquid chromatography; Fmoc, N-(9-fluorenyl)methoxycarbonyl; SPR, surface plasmon resonance.

were transiently transfected with SuperFect (Qiagen, Valencia, CA). After incubation for 24 h, the cells were washed twice with phosphate-buffered saline and lysed in 1% Triton X-100 lysis buffer (20 mM Tris-HCl, pH 7.5, 25 mM NaF, 12.5 mM Na₄P₂O₇, 0.1 mM EDTA, 50 mM NaCl, 2 mM Na₃VO₄, and protease inhibitors). After centrifugation (15,000 × *g*, 15 min, 4 °C) to remove cellular debris, the supernatant was subjected to an ultracentrifugation (100,000 × *g*) for 30 min. Equal amounts of total protein were incubated for 1 h at 4 °C with anti-FLAG M2-agarose (Sigma). The beads were washed extensively with lysis buffer.

Preparation of Samples for Mass Spectrometry—Immuno-precipitates were separated on SDS-polyacrylamide gels and stained with GelCode Blue Colloidal Coomassie reagent (MJS BioLynx Inc., Brockville, ON, Canada) as previously described (22). Silver staining of gels was performed as described by Shevchenko *et al.* (23). Individual bands were excised from the gel with a scalpel and placed into a single well of a 96-well microtitre plate (Genomic Solutions, Ann Arbor, MI). Reduction, alkylation, and “in-gel” tryptic digestion of samples was performed with a Genomic Solutions ProGest digestion robot as previously described (24). Tryptic peptides were then extracted from the gel for analysis by mass spectrometry.

Liquid Chromatography-Tandem Mass Spectrometry—Tryptic peptides were analyzed by liquid chromatography-tandem mass spectrometry with a HP 1100 HPLC system (Palo Alto, CA) connected to an LCQ-Deca mass spectrometer (Thermo Electron, San Jose, CA) as previously described (22). Data were analyzed with both the Mascot (4) and Sonar ms/ms (Genomic Solutions) search engines.

Plasmids—Glutathione *S*-transferase (GST) fusion proteins were made using the PGEX-KG vector (25). A DNA fragment encoding the COOH-terminal CD2AP (residues 324–636) was cloned in-frame into vector cut with BamHI and EcoRI. Sequences encoding a COOH-terminal fragment of CD2AP lacking the proline-rich sequence CTΔPR (residues 424–636) was amplified by PCR using *Pfu* polymerase (Stratagene) and cloned in-frame into the NcoI and Sall sites of PGEX-KG. The COOH-terminal construct lacking the coiled-coil domain CTΔCC (residues 424–588) was generated by deletion mutagenesis of residues encoding 589–636. Constructs encoding residues 424–528 and 474–588 were generated by deletion mutagenesis of CTΔPR. The construct encoding residues 474–528 was generated by deletion mutagenesis using the construct encoding residues 478–592 as the starting point. The construct encoding residues 474–528 was used to generate constructs with residues 474–513, 474–598, 490–528, and 506–528 by deletion mutagenesis. Point mutations in CTΔPR (L486A, H488A, T490A, N492A, R493A, K495A, R500A, and P502A) were generated by site-directed mutagenesis by PCR.

Proteins—GST fusion proteins were expressed in *Escherichia coli* and affinity-purified using standard procedures using glutathione-agarose (Sigma). Chicken-capping protein CP α_1 and β_1 subunits were co-expressed in *E. coli* using the pET-3d vector and purified as described previously (16). The CP deletion mutants $\alpha_1\Delta\beta_1$ (α_1 COOH-terminal 28-amino-acid deletion mutant), $\alpha_1\beta_1\Delta$ (β_1 COOH-terminal 34-amino-acid deletion mutant), and

$\alpha_1\Delta\beta_1\Delta$ (double COOH-terminal region deletion mutant) were purified as described in Ref. 16.

Confirmatory sequencing of all constructs was done using Big-Dye 3.1 (Applied Biosystems). Purified proteins were analyzed by SDS-PAGE and Coomassie staining. Protein concentrations were estimated using the BCA protein assay (Pierce) and by absorbance measurement at 280-nm wavelength.

BIAcore Analysis—The experiments were carried out using a BIAcore 2000 at 25 and 30 °C for both binding detection and affinity measurements. Goat anti-GST antibody (BIAcore, Uppsala, Sweden) was cross-linked to CM5 chips using amine coupling (BIAcore). CD2AP constructs fused to GST were then loaded onto chips containing the immobilized anti-GST antibody in a buffer containing 10 mM Hepes, pH 7.4, 150 mM NaCl, 4 mM EDTA, and 0.005% Tween 20. CP was injected at various concentrations at a flow rate of 25 μ l/min.

To measure the affinity by Scatchard analysis, CP was injected at various concentrations, and the equilibrium binding was obtained and plotted. The binding kinetic rate constants were obtained by using BIAevaluation version 3.1 software (BIAcore). The k_{off} rate was measured by co-injecting soluble CD2AP during the dissociation phase of the reaction.

To compare the binding of various mutated constructs, similar amounts of GST-CD2AP constructs were captured on the chip. Because the magnitude of the response is related to the mass of the analyte, we corrected for differences in the molecular weights of each construct and variances in the amount immobilized on the chip using the equation $RU_{max} = RU_{ligand} \times (\text{molecular weight of analyte/molecular weight of ligand})$. This allowed us to calculate a relative RU_{max} for each construct. The percent binding of the mutated construct in comparison to the wild-type construct was then computed by comparing the actual RU of the bound CP at steady state (R_{eq}) to the calculated R_{max} .

Peptides—The 22-mer peptides used for the competition assay were synthesized by standard Fmoc chemistry using a multiple peptide synthesizer (Symphony/Multiplex; Protein Technologies, Tucson, AZ). All peptides were purified by HPLC, and their sequences were verified by mass spectrometry. The sequences of the peptides used were: CARMIL, RRLEHT-KLRPKRNKKQQTQA; CKIP-1, SYLAHPTDRAKIQHSR-RPPTR; CD2AP, ENLLHLTANRPKMPGRRRLPGRF; and CD2AP (R493A), ENLLHLTANAPKMPGRRRLPGRF (the bold letter indicates the mutation).

Spectrin F-actin-seeded Actin Polymerization Assay—Proteins and spectrin F-actin seeds were prepared and assayed as described in Ref. 16. Actin was used at a final concentration of 1.5 μ M (3% pyrene-labeled) in 1× polymerization buffer (10 mM Tris-HCl, pH 7.5, 50 mM KCl, 1 mM MgCl₂, 0.2 mM ATP, 0.5 mM dithiothreitol, 0.2 mM CaCl₂, and 1 mM EGTA). Ca²⁺-G-actin was primed for 90 s prior to the initiation of polymerization by adding a 1/10 volume of 10 mM EGTA, 1 mM MgCl₂ to exchange Ca²⁺ to Mg²⁺. A 1/20 volume of 20× polymerization buffer (200 mM Tris-HCl, pH 7.5, 1 M KCl, 20 mM MgCl₂, and 20 mM EGTA) was then added to initiate polymerization. CP, GST-CD2AP (CTΔPR), and GST-CD2AP-(474–513) were in 10 mM Tris-HCl, pH 7.5, 50 mM KCl, 1 mM MgCl₂, 0.5 mM dithiothreitol, and 1 mM EGTA. The CP and CP-CD2AP mixtures were

Identifying a Novel Actin-capping Protein Binding Motif

added to the actin mixture immediately after priming, followed by the addition of 20× polymerization buffer, followed by 10 μl of spectrin F-actin seed. The solution was mixed and placed in the fluorometer with a total dead time of 20 s. The solution was then recovered and incubated overnight at 25 °C to reach equilibrium to allow for measurements at steady state. The steady-state binding data were analyzed using PRISM4 software.

Actin Uncapping Assay—The uncapping assay was a modification of the actin polymerization assay using 1 μM actin (5% pyrene-labeled) and 2 nM CP. It was performed essentially as described in Ref. 26. Uncapping activity is defined as the rate of polymerization, calculated from the slope of the pyrene fluorescence *versus* time, following the addition of CARMIL or CD2AP-(474–513).

RESULTS

Identification of CD2AP-associated Protein by Mass Spectrometry—To identify CD2AP-interacting proteins, an epitope-tagged version of CD2AP was overexpressed in HEK293 cells and immunoprecipitated. The co-precipitated proteins were analyzed by SDS-PAGE and silver staining. The identification of protein bands was performed using mass spectrometry. In addition to CD2AP, several previously described CD2AP-interacting proteins were identified, such as actin (27), cortactin (12), and actin-capping protein CP (11). Novel interacting partners were also identified. These included Cin85 (4, 5), tensin (28), clathrin adaptor protein 2, two Rho and Rac GTPase-activating proteins centaurin δ2 (29) and SH3BP1 (30), synaptojanin 2 (31), glial fibrillary acidic protein (GFAP), RNA-binding protein 10, heat shock protein (HSP70), and breast cancer type 1-susceptible protein (BRCA1) (32).

The identification of multiple proteins involved in actin cytoskeletal regulation suggested that CD2AP participates in the regulation of the actin cytoskeleton. Because CP plays an important role in the assembly of various actin structures, we hypothesized that CD2AP might regulate the activity of CP. We therefore focused on characterizing the interaction of CP with CD2AP in more detail.

Mapping the Interaction Domain—Previously, an interaction of CP with the COOH-terminal half of CMS (Cas ligand with multiple SH3 domains), the human ortholog of CD2AP, was reported (11). To confirm this, we generated a GST fusion protein containing residues 324–636 of CD2AP and tested it for interaction with purified CP using surface plasmon resonance (SPR). CD2AP was immobilized on the chip, and CP was used as the analyte. As predicted, the fragment encoding the COOH-terminal half of CD2AP interacted with CP (Fig. 1B). Scatchard analysis showed that this fragment bound to CP with a dissociation constant (K_D) of 2.4 nM. Real-time measurements revealed binding kinetics of $k_{on} = 9.6 \times 10^5 \text{ M}^{-1} \text{ s}^{-1}$ and $k_{off} = 2.3 \times 10^{-3} \text{ s}^{-1}$ (Fig. 1C).

The COOH-terminal half of CD2AP is notable for proline-rich sequences followed by a predicted coiled-coil domain near the extreme COOH terminus (1). We first tested the requirement of the coiled-coil domain for binding to CP by generating a construct lacking the coiled-coil domain CTΔCC (residues 324–588). Using SPR, we found that this construct still bound

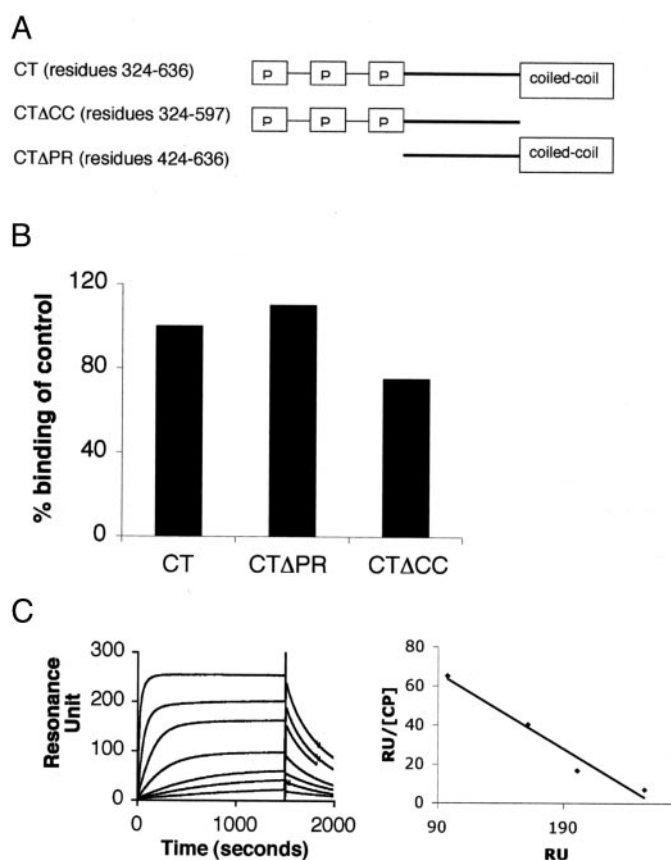


FIGURE 1. CP requires neither the proline-rich sequence nor the coiled-coil domain of CD2AP for binding. A, schematic representation of the COOH-terminal domains of CD2AP. B, CD2AP lacking the proline-rich sequence and the coil-coil domain bind CP. Constructs encoding fragments of CD2AP lacking the proline-rich sequence (CTΔPR) or lacking the coiled-coil domain (CTΔCC) were generated by PCR and expressed in bacteria. The interaction between CD2AP constructs and CP was measured using surface plasmon resonance. The CD2AP constructs were immobilized on the chip using a GST capturing kit protocol. GST alone in a separate flow cell was used as a negative control (CT) test for an interaction, and CP (50 nM) was injected onto the chip. The binding of the control was set to 100%. Each analysis was corrected for differences in the molecular weight and for variances in initial immobilization as described under "Experimental Procedures." C, CP binds to CD2AP with a high affinity. Increasing amounts of CP (0.1, 0.3, 0.5, 1.5, 4, 12, and 36 nM) were injected over immobilized CTΔPR to measure the binding affinity. BIAevaluation analysis was carried out to determine the binding rate constants ($k_{on} = 9.6 \times 10^5 \text{ M}^{-1} \text{ s}^{-1}$, $k_{off} = 2.3 \times 10^{-3} \text{ s}^{-1}$). The binding affinity was calculated to be 2.4 nM using Scatchard plot analysis. RU, resonance units.

to CP. Therefore, the coiled-coil domain is not required for binding (Fig. 1B).

Next, we tested whether the proline-rich sequences of CD2AP were required for binding. A construct, CTΔPR (residues 428–636), lacking the proline-rich sequences between 324 and 428, was generated and tested for its ability to bind CP by SPR. This construct also retained binding to CP, suggesting that the proline-rich sequences were not required for binding (Fig. 1B). Therefore, we deduced that the region of CD2AP between the proline-rich sequences and the coiled-coil domain (residues 424–588) contains the CP binding region.

To define the interaction site further, we generated additional truncation mutants. Because this region has no predicted secondary structure, we generated constructs eliminating either 60 residues from the COOH terminus (residues 424–

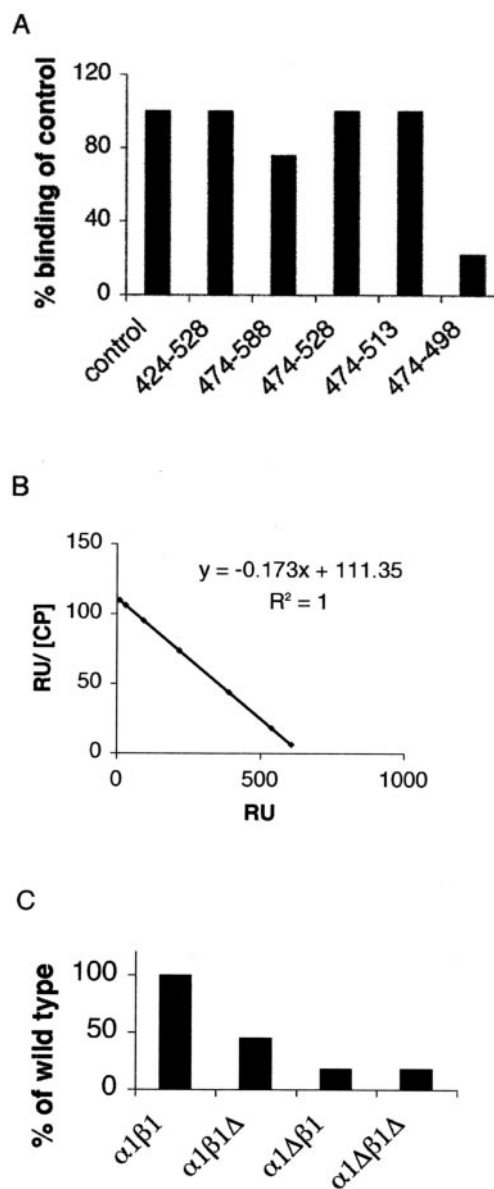


FIGURE 2. Defining minimal CD2AP and CP binding domains. *A*, various truncation mutants of CD2AP were tested for CP binding using SPR. Each construct was generated by PCR mutagenesis and expressed as fusion proteins in bacteria. Purified proteins were immobilized on the chip, and CP binding was assessed as described in the legend to Fig. 1. *B*, the region 474–513 is sufficient to bind CP with high affinity. A fragment containing residues 474–513 was immobilized on the BIAcore chip. A range of concentrations of CP (0.1, 0.3, 1, 3, 9, 30, and 100 nM) was injected onto the chip. Scatchard analysis generated an affinity of 5.6 nM. BIAevaluation analysis generated binding rate constants of $k_{on} = 4.67 \times 10^5 \text{ M}^{-1} \text{ s}^{-1}$ and $k_{off} = 2.6 \times 10^{-3} \text{ s}^{-1}$. *RU*, resonance units. *C*, various truncation mutants of CP were tested for CD2AP binding. CTAPR was immobilized to the chip, and 50 nM α COOH-terminal region, β COOH-terminal region, and $\alpha\beta$ double COOH-terminal regions deletion mutants of CP were tested for CD2AP binding using SPR.

528) or 50 residues from the NH₂-terminal end (residues 474–588). Both constructs retained binding to CP (Fig. 2A), narrowing the binding region to residues 474–528.

The region 474–528 was sufficient for binding, because a construct encoding just these residues was able to bind to CP measured by SPR (Fig. 2A). We narrowed the binding site further by generating additional constructs, deleting residues from both the NH₂ and COOH termini. Although the construct

encoding residues 474–513 retained binding to CP, the construct encoding residues 474–498 had impaired binding. Thus, residues between 474 and 513 were sufficient for CP binding (Fig. 2A).

We measured the binding affinity of this minimal binding region of CD2AP (residues 474–513) with CP. Scatchard analysis showed that CD2AP bound to CP with a K_D of 5.6 nM, and real-time measurements showed binding kinetics of $k_{on} = 4.7 \times 10^5 \text{ M}^{-1} \text{ s}^{-1}$ and $k_{off} = 2.6 \times 10^{-3} \text{ s}^{-1}$ (Fig. 2B). Because this affinity is similar to the one measured for the interaction of the entire COOH-terminal half of CD2AP with CP, this region was sufficient to account for CP binding.

CP is a heterodimer of α and β subunits. The COOH termini of both subunits are known to be important for its actin-capping activity (16). To test the importance of these regions for the interaction with CD2AP, CP constructs lacking the α COOH-terminal region, the β COOH-terminal region, or both were tested for binding to CTAPR. CP lacking the α COOH-terminal region or both the α and β COOH termini regions did not interact with CD2AP, whereas CP lacking just the β COOH-terminal region had an intermediate binding ability (Fig. 2C). Hence, CD2AP requires both α and β COOH termini regions of CP for efficient binding. These results predicted that CD2AP should inhibit capping activity of CP.

Identification of CP Binding Motif—Recently, the binding regions for two CP-binding proteins, CKIP and CARMIL, were reported (18, 20). To determine whether these binding sites had similarities to residues 474–513 of CD2AP, we performed a CLUSTAL analysis. The sequence alignment illustrated in Fig. 3A shows that all three proteins share a similar pattern of residues, LXHXTXXRPK(X)₆P (where X is any amino acid) suggesting that this may be the CP binding motif.

To determine whether the residues in this motif are important for CP binding, we mutated each of the conserved residues to alanine in the CTAPR construct (residues 428–636). Each mutant was tested for CP binding using SPR (Fig. 3B). Mutation of the conserved leucine, arginine, and proline residues (Lue-486, Arg-493, Pro-502) completely ablated binding, whereas mutations of the other conserved residues significantly impaired but did not completely ablate binding. Importantly, mutations of two non-conserved residues in CD2AP, N492 and R500, did not affect binding of CP to CD2AP. Therefore, we concluded that the LXHXTXXRPK(X)₆P motif in CD2AP is necessary for binding.

To verify that the LXHXTXXRPK(X)₆P motif found in all three proteins (CD2AP, CARMIL, and CKIP-1) is the binding site, we tested 22-mer peptides corresponding to this motif from CKIP-1 and CARMIL in a competition assay against the CD2AP protein. The ability of the CKIP-1 and CARMIL peptides to inhibit CD2AP binding to CP (Fig. 3C) confirmed that all three of these proteins use this motif to bind to CP, and therefore this motif is sufficient for binding.

Inhibition of CP Activity by CD2AP—Because both the actin-capping activity and CD2AP binding required the COOH-terminal regions of CP, we were interested to test whether CD2AP binding could affect CP-capping activity. This was tested using a pyrene-actin polymerization assay for barbed end growth *in vitro* as described under “Experimental Procedures.” The

Identifying a Novel Actin-capping Protein Binding Motif

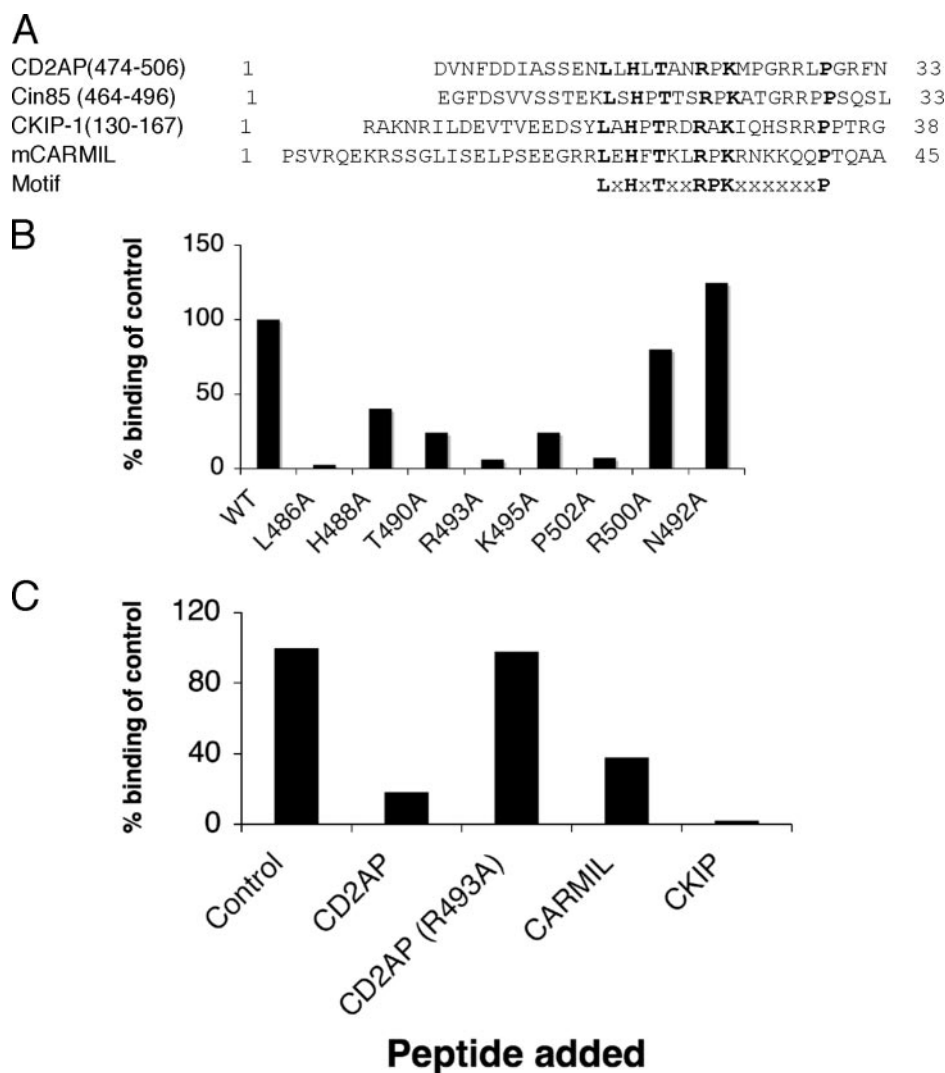


FIGURE 3. Identification of CP binding motif. *A*, CLUSTAL analysis of CD2AP, Cin85, CKIP-1, and mCARMIL. The residues conserved within these proteins are *highlighted in bold*. The proposed motif is shown *underneath*. The one-letter amino acid representation is used. *X* represents any amino acid. *B*, identification of critical binding site residues. Each of the conserved residues defined in *A* was mutated to alanine using site-directed mutagenesis. In addition, two of the non-conserved residues (Arg-500 and Asn-492) were mutated as a negative control. Each mutated construct was expressed in bacteria, purified, and tested for binding to CP. Each analysis was corrected for differences in the molecular weight and for variances in initial immobilization as described under "Experimental Procedures." *WT*, wild type. *C*, synthetic peptides derived from CD2AP, CKIP-1, and CARMIL compete for binding to CP. Peptides corresponding to the putative CP binding site in CD2AP, CKIP-1, and CARMIL were synthesized using standard Fmoc chemistry. The sequence of the 22-mer peptides is given under "Experimental Procedures." SPR was used to measure the ability of peptides to inhibit the binding of CP to CD2AP. Briefly, 50 nM CP was incubated with 1 μ M peptide and injected. As a negative control, a peptide derived from CD2AP with Arg-493 changed to alanine was also tested.

polymerization of pyrene-actin as assessed by its fluorescence was measured over time. The addition of up to 500 nM CT Δ PR alone to the reaction mixture did not have any effect on actin polymerization, and as expected, the addition of CP inhibited barbed end growth. Addition of CT Δ PR to CP inhibited the activity of CP in a concentration-dependent manner (Fig. 4A). A similar effect was observed with the addition of the minimal binding domain (residues 474–513) (data not shown). The inhibitory effect of CD2AP on the activity of CP was saturated when the CT Δ PR concentration reached \sim 500 nM (Fig. 4A). Because this is much higher than the K_D of CP for CD2AP, we suggest that the inhibition of CP by CD2AP is not complete.

The partial inhibitory effect of CD2AP on CP actin-capping activity was confirmed using a steady-state polymerization assay. In this experiment, the effect of CD2AP was allowed to go to equilibrium by allowing the reaction to go to completion; actin fluorescence was measured after 18 h. Using PRISM4 software, the affinity of CD2AP for CP was found to be similar to that measured by SPR (Fig. 4B). In addition, because the activity of CP was not completely inhibited, this suggests that the CD2AP-CP complex still retains some filament-capping activity. As shown in Fig. 4B, after the complex had reached equilibrium, full actin polymerization had not been achieved, suggesting that the CD2AP-CP complex retains a low but detectable affinity for the barbed end. Taken together, the results show that CD2AP partially inhibits the capping activity of CP and that the CP-CD2AP complex has the ability to cap the barbed end but at a much slower rate.

The ability of CD2AP to uncapping actin filaments was also tested (Fig. 4C). 500 nM CD2AP-(474–513) was added to actin polymerization reactions containing CP at a time when most of the barbed ends were already capped. The addition of CD2AP-(474–513) resulted in increased actin polymerization, consistent with the dissociation of CP from F-actin.

DISCUSSION

In this report, we present data supporting the role of CD2AP as a regulator of the actin cytoskeleton. In a proteomic screen, we identified several actin regulatory proteins associated with CD2AP, including actin capping protein, cortactin, and synaptojanin. By mapping its interaction with CP, we identified a novel motif in CD2AP that is also found in Cin85, CKIP-1, and CARMIL that mediates binding to CP. Because CD2AP inhibits the activity of CP, the interaction between CP and CD2AP appears to be functionally relevant.

In the proteomic screen, we identified known CD2AP-interacting proteins, including capping protein and cortactin (11, 12). Synaptojanin is reported to bind to Cin85 but has not yet been reported to bind to CD2AP (7). We also identified new CD2AP-binding proteins. Although the clathrin adaptor protein 2 was implicated as a CD2AP-interacting protein because of the presence of the FXDXF binding motif (9), this is the first

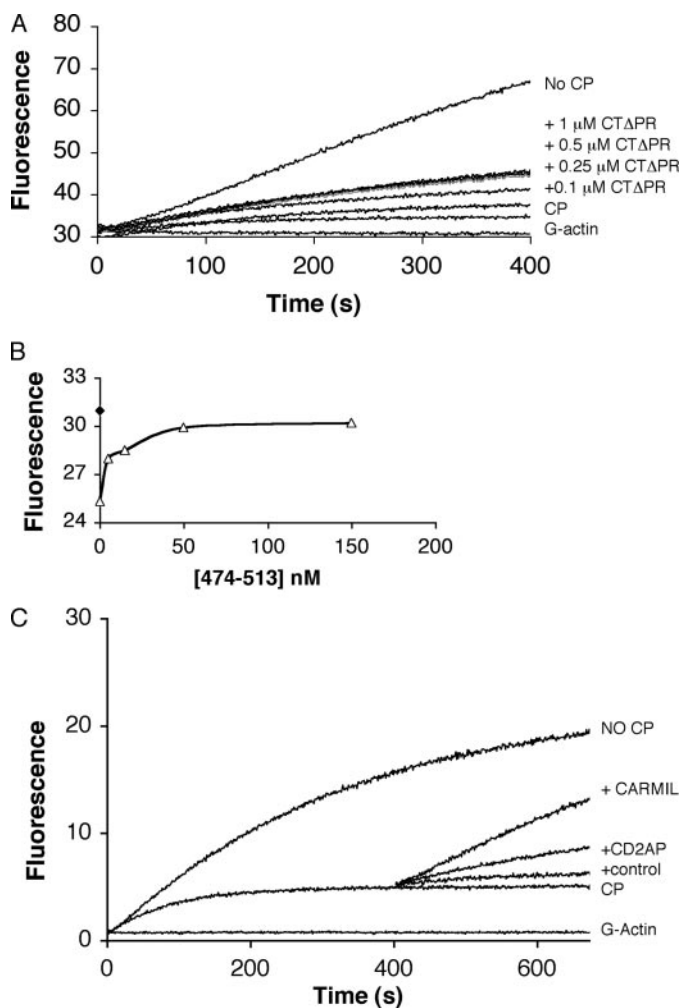


FIGURE 4. CD2AP inhibits CP and also exhibits uncapping activity. A, CD2AP inhibits CP activity. Actin polymerization was measured using a fluorescence-based pyrene-actin assay. Spectrin actin seeds were used to initiate actin polymerization. CP (4 nM) was added by itself or after preincubation with CTΔPR at the indicated concentrations. B, the binding affinity of CP and CD2AP was determined from steady-state F-actin polymerization measurements. To a solution containing 1.5 μM actin and spectrin F-actin seeds (filled diamond), 5 nM CP with or without increasing amounts of CD2AP-(474–513) (5, 15, 50, and 150 nM) were added. Samples were incubated overnight to reach equilibrium before fluorescence measurement. C, CD2AP promotes the dissociation of CP from actin filaments. Actin polymerization was initiated as described for *a* and *b* with spectrin F-actin seed and the addition of CP (2 nM). After 400 s, 500 nM CD2AP-(474–513) or 40 nM CARMIL was added. An equal volume of buffer alone was also added as a negative control. Actin polymerization was measured using a fluorometer.

demonstration that CD2AP can, in fact, bind to it. Other novel interactions include centaurin δ2 and SH3BP1, which are GTPase-activating proteins for the Rho and Rac GTPases, respectively (29, 30). We also identified tensin, a focal adhesion protein with multiple actin binding domains, which is a known inhibitor of actin polymerization (28). On the other hand, we did not find other reported CD2AP-binding proteins, such as Fyn, Src, Yes, or the p85 regulatory subunit of phosphatidylinositol 3-kinase (33). This might be because these proteins have a transient or low affinity interaction with CD2AP. It is also possible that the conditions we used in our screen did not favor their binding to CD2AP. We also identified other proteins of unknown significance, such as RNA-binding protein 10, glial

fibrillary acidic protein, and the breast and ovarian cancer susceptibility protein BRCA1 (32). Further work will be needed to determine the significance of these interactions.

To better define the CD2AP/CP interaction, we mapped the minimal binding region of CD2AP to amino acids 474–513. This domain does not have any predicted secondary structure and is located between the proline-rich sequences and coiled-coil domain at the COOH terminus. Using a CLUSTAL analysis to compare this sequence to the sequences of two other known CP-binding proteins, CKIP-1 and CARMIL, we identified the novel motif LXHXTXXRPK(X)₆P. This motif is also found in Cin85. Since the original submission of the manuscript of this article, Urono *et al.* (34) report that a conserved sequence similar to the motif we describe is present in all known forms of CARMIL.

Mutations of all of the conserved residues showed that they are important for binding, with Leu-486, Arg-493, and Pro-502 being the most critical residues. Consistent with our findings, mutation of the analogous arginine in CARMIL was recently shown to be important for CP binding (20). Pro-494 of CD2AP is conserved in Cin85 and CARMIL; however, it is alanine in CKIP-1. In the peptide competition assay, CKIP-1 bound to CP better than CARMIL, suggesting that an alanine residue at this position might enhance binding. To address this, we generated a mutated construct with alanine substituted for proline in CD2AP and tested its ability to bind to CP. Surprisingly, this construct had ~50% lower binding compared with wild-type CD2AP (data not shown). This result confirmed that the conserved proline in CD2AP is important for binding and demonstrates that the binding difference between CKIP-1 and CD2AP is not due to the alanine residue. The higher affinity of CKIP-1, however, does suggest that there is a level of complexity of the binding that goes beyond the binding motif that we identified here. It is interesting to note that the residues between Lys-495 and Pro-502 are mainly basic residues. These residues might play important roles in modulating binding.

We searched the data base for other proteins containing this motif but did not identify any others. Although it is possible that these four proteins are the only molecules containing this motif, it seems more likely that variants of this motif exist. Nevertheless, our peptide competition studies demonstrate that this motif is used similarly by CD2AP, CKIP-1, and CARMIL to bind to CP.

The COOH termini of both the α and β subunits of CP are important for its capping activity (16), and they were also important for CD2AP binding. The interaction of CARMIL with CP, however, did not require either the α or β COOH termini regions of CP for binding (20). Because the fragment of CARMIL used was much larger than the portion of CD2AP tested here, this suggests that CARMIL might interact with other regions of CP in addition to the area that was defined here. Mapping studies with CARMIL will be required to determine whether additional interacting sites exist.

Because the β COOH-terminal region was involved in CD2AP binding, and the β₁ and β₂ isoforms differ in this region (35), we tested whether the CD2AP interaction with CP was β isoform-specific. The two isoforms of CP (α₁β₁, α₁β₂) had similar binding affinities to CD2AP (data not

Identifying a Novel Actin-capping Protein Binding Motif

shown). This suggests that CD2AP interacts with conserved residues within the COOH-terminal regions of the β_1 and β_2 isoforms or that the specific sequence of the β COOH terminus is not important.

Our data suggest that CD2AP can regulate actin dynamics by partially inhibiting CP and/or by promoting uncapping of the barbed end. Similar to CARMIL, we found that CD2AP does not completely block the capping activity of CP (20). At saturating amounts of CD2AP, some capping activity of CP was still retained. Although this may be secondary to the fact that we tested only fragments of CD2AP rather than the full-length protein, we are intrigued by the possibility that CD2AP binding to CP may function to modulate and not completely inhibit its activity. Because the concentration of CP and CD2AP in cells (estimated in the μM range) is far above the affinity of CP for the barbed ends, the CP·CD2AP complex is likely to retain significant capping activity *in vivo*. With the growing number of identified CP-binding proteins, the potential for each to change the binding affinity of CP in different ways may allow for a broader diversity of actin filament structures.

This might not be the only way CD2AP regulates the actin cytoskeleton. Similar to CARMIL, we found that CD2AP can uncap barbed end filaments (18, 20). CD2AP joins CARMIL as the only known proteins able to uncap barbed ends. Given the high affinity of CD2AP for CP, it would be expected that much of the CP would be bound to CD2AP in the cell. However, given the increasing number of identified CP-binding proteins, it seems more likely that distinct pools of CP exist bound to different CP-binding proteins. Because CD2AP and its homolog Cin85 can form heterodimers mediated by their coiled-coil domain³ and both can bind to CP, it is very likely that they form a ternary complex in cells. It will be interesting to determine how these complexes are regulated *in vivo*, because CD2AP is associated with other actin regulatory proteins such as cortactin (12). The role of CD2AP in actin regulation could be complex. We are interested to determine what roles CD2AP plays in regulating other modes of actin polymerization.

Recently, Mejillano *et al.* (36) have demonstrated that the balance between filopodia and lamellopodia is dependent on CP. When CP expression is inhibited using RNA interference, long unbranched actin filaments are favored over short branched actin filaments. Thus, it is conceivable that recruitment of CD2AP to the plasma membrane might inhibit CP activity and thereby function to enhance filopodia formation or decrease the density of branched filaments. However, we were unable to confirm this hypothesis in cells. Phalloidin analysis of CD2AP-deficient cells compared with wild-type cells did not show any differences nor did motility studies (data not shown). In addition, clustering of a COOH-terminal fragment of CD2AP (containing the capping binding site) to the plasma membrane did not induce any local filopodia. Overexpression of full-length CD2AP also had no obvious effect on the actin cytoskeleton. Although the presence of Cin85 could be a confounding factor in our experi-

ments, these results suggest that CD2AP-dependent changes in the actin cytoskeleton cannot account for the podocyte defect responsible for renal failure. We are, however, continuing to investigate whether the actin and adhesion molecule dynamics is affected by CD2AP.

Acknowledgments—We thank Dr. Joseph Lin for reading the manuscript and Dr. Nandini Bhattacharya for sharing reagents.

REFERENCES

1. Dustin, M. L., Olszowy, M. W., Holdorf, A. D., Li, J., Bromley, S., Desai, N., Widder, P., Rosenberger, F., van der Merwe, P. A., Allen, P. M., and Shaw, A. S. (1998) *Cell* **94**, 667–677
2. Shih, N. Y., Li, J., Karpitskii, V., Nguyen, A., Dustin, M. L., Kanagawa, O., Miner, J. H., and Shaw, A. S. (1999) *Science* **286**, 312–315
3. Shih, N. Y., Li, J., Cotran, R., Mundel, P., Miner, J. H., and Shaw, A. S. (2001) *Am. J. Pathol.* **159**, 2303–2308
4. Take, H., Watanabe, S., Takeda, K., Yu, Z. X., Iwata, N., and Kajigaya, S. (2000) *Biochem. Biophys. Res. Commun.* **268**, 321–328
5. Gout, I., Middleton, G., Adu, J., Ninkina, N. N., Drobot, L. B., Filonenko, V., Matsuka, G., Davies, A. M., Waterfield, M., and Buchman, V. L. (2000) *EMBO J.* **19**, 4015–4025
6. Cormont, M., Meton, I., Mari, M., Monzo, P., Keslair, F., Gaskin, C., McGraw, T. E., and Le Marchand-Brustel, Y. (2003) *Traffic* **4**, 97–112
7. Kowanez, K., Husnjak, K., Holler, D., Kowanez, M., Soubeyran, P., Hirsch, D., Schmidt, M. H., Pavelic, K., De Camilli, P., Randazzo, P. A., and Dikic, I. (2004) *Mol. Biol. Cell* **15**, 3155–3166
8. Soubeyran, P., Kowanez, K., Szymkiewicz, I., Langdon, W. Y., and Dikic, I. (2002) *Nature* **416**, 183–187
9. Brett, T. J., Traub, L. M., and Fremont, D. H. (2002) *Structure (Camb.)* **10**, 797–809
10. Liu, Y., Yerushalmi, G. M., Grigera, P. R., and Parsons, J. T. (2005) *J. Biol. Chem.* **280**, 8884–8892
11. Hutchings, N. J., Clarkson, N., Chalkley, R., Barclay, A. N., and Brown, M. H. (2003) *J. Biol. Chem.* **278**, 22396–22403
12. Lynch, D. K., Winata, S. C., Lyons, R. J., Hughes, W. E., Lehrbach, G. M., Wasinger, V., Corthals, G., Cordwell, S., and Daly, R. J. (2003) *J. Biol. Chem.* **278**, 21805–21813
13. Cooper, J. A., and Schafer, D. A. (2000) *Curr. Opin. Cell Biol.* **12**, 97–103
14. Harris, E. S., and Higgs, H. N. (2004) *Curr. Biol.* **14**, R520–R522
15. Cooper, J. A., Blum, J. D., and Pollard, T. D. (1984) *J. Cell Biol.* **99**, 217–225
16. Wear, M. A., Yamashita, A., Kim, K., Maeda, Y., and Cooper, J. A. (2003) *Curr. Biol.* **13**, 1531–1537
17. Pollard, T. D., and Beltzner, C. C. (2002) *Curr. Opin. Struct. Biol.* **12**, 768–774
18. Canton, D. A., Olsten, M. E., Kim, K., Doherty-Kirby, A., Lajoie, G., Cooper, J. A., and Litchfield, D. W. (2005) *Mol. Cell. Biol.* **25**, 3519–3534
19. Taoka, M., Ichimura, T., Wakamiya-Tsuruta, A., Kubota, Y., Araki, T., Obinata, T., and Isobe, T. (2003) *J. Biol. Chem.* **278**, 5864–5870
20. Yang, C., Pring, M., Wear, M. A., Huang, M., Cooper, J. A., Svitkina, T. M., and Zigmund, S. H. (2005) *Dev. Cell* **9**, 209–221
21. Huber, T. B., Hartleben, B., Kim, J., Schmidts, M., Schermer, B., Keil, A., Egger, L., Lecha, R. L., Borner, C., Pavenstadt, H., Shaw, A. S., Walz, G., and Benzing, T. (2003) *Mol. Cell. Biol.* **23**, 4917–4928
22. Ingham, R. J., Colwill, K., Howard, C., Dettwiler, S., Lim, C. S., Yu, J., Hersi, K., Raaijmakers, J., Gish, G., Mbamalu, G., Taylor, L., Yeung, B., Vassilovski, G., Amin, M., Chen, F., Matskova, L., Winberg, G., Ernberg, I., Lindring, R., O'Donnell, P., Starostine, A., Keller, W., Metalnikov, P., Stark, C., and Pawson, T. (2005) *Mol. Cell. Biol.* **25**, 7092–7106
23. Shevchenko, A., Wilm, M., Vorm, O., and Mann, M. (1996) *Anal. Chem.* **68**, 850–858
24. Houthaeve, T., Gausepohl, H., Mann, M., and Ashman, K. (1995) *FEBS Lett.* **376**, 91–94
25. Guan, K. L., and Dixon, J. E. (1991) *Anal. Biochem.* **192**, 262–267

³ T. B. Huber and A. S. Shaw, unpublished data.

26. Schafer, D. A., Jennings, P. B., and Cooper, J. A. (1996) *J. Cell Biol.* **135**, 169–179
27. Lehtonen, S., Zhao, F., and Lehtonen, E. (2002) *Am. J. Physiol.* **283**, F734–F743
28. Lo, S. H., Janmey, P. A., Hartwig, J. H., and Chen, L. B. (1994) *J. Cell Biol.* **125**, 1067–1075
29. Miura, K., Jacques, K. M., Stauffer, S., Kubosaki, A., Zhu, K., Hirsch, D. S., Resau, J., Zheng, Y., and Randazzo, P. A. (2002) *Mol. Cell* **9**, 109–119
30. Cicchetti, P., Ridley, A. J., Zheng, Y., Cerione, R. A., and Baltimore, D. (1995) *EMBO J.* **14**, 3127–3135
31. McPherson, P. S., Garcia, E. P., Slepnev, V. I., David, C., Zhang, X., Grabs, D., Sossin, W. S., Bauerfeind, R., Nemoto, Y., and De Camilli, P. (1996) *Nature* **379**, 353–357
32. Bowcock, A. M. (1993) *Breast Cancer Res. Treat.* **28**, 121–135
33. Kirsch, K. H., Georgescu, M. M., Ishimaru, S., and Hanafusa, H. (1999) *Proc. Natl. Acad. Sci. U. S. A.* **96**, 6211–6216
34. Uruno, T., Remmert, K., and Hammer, J. A., III (2006) *J. Biol. Chem.* **281**, 10635–10650
35. Hart, M. C., and Cooper, J. A. (1999) *J. Cell Biol.* **147**, 1287–1298
36. Mejillano, M. R., Kojima, S., Applewhite, D. A., Gertler, F. B., Svitkina, T. M., and Borisy, G. G. (2004) *Cell* **118**, 363–373